

# A Photoelectrochemical Sensor for the Sensitive Detection of Rutin Based on a CdSe QDs Sensitized TiO<sub>2</sub> Photoanode

Liyang Wei, Xiaokun Li\*, Suxiang Feng

College of Pharmacy, Henan University of Chinese Medicine, Zhengzhou 450046, China

\*E-mail: [li96052122@126.com](mailto:li96052122@126.com)

*Received:* 1 October 2020 / *Accepted:* 4 November 2020 / *Published:* 30 November 2020

---

In this paper, a CdSe quantum dots (QDs) sensitized TiO<sub>2</sub> photoanode was synthesized by molten-salt-assisted self-assembly (MASA) on a fluorine-doped tin oxide (FTO)-coated glass (CdSe QDs-TiO<sub>2</sub>/FTO), and an efficient photoelectrochemical (PEC) sensor was constructed for the sensitive detection of rutin. CdSe can transfer photo-excited electrons to the conduction band of TiO<sub>2</sub>, thus enhancing the photoelectric activity of TiO<sub>2</sub>. The experimental results show that the PEC sensor has excellent selectivity, good stability, and a wide linear response range for rutin of 0.025–50.0 μM with a low detection limit of 0.007 μM. Moreover, the PEC sensor was successfully applied to the detection of rutin content in serum sample.

---

**Keywords:** Photoelectrochemical sensor; CdSe QDs; TiO<sub>2</sub>; molten-salt-assisted self-assembly; rutin

## 1. INTRODUCTION

Rutin (3',4',5,7-tetrahydroxyflavone-3-d-rutinoside), also known as Vitamin P, is a flavonol glycoside comprised of the flavonol quercetin and the disaccharide rutinose (Figure 1) [1]. It is an important natural flavonoid and is widely found in buckwheat plants [2,3]. Rutin has antioxidant, anti-inflammatory, antibacterial, anti-diabetes, and free radical scavenging activities and can be used to treat hypertension and diabetes [4-7]. Based on these good properties, rutin is widely used in medicine, health food, and cosmetics and has high development value. Therefore, a simple, rapid, and sensitive method for detecting rutin should be developed. Many analytical methods have been applied for the detection of rutin, including high-performance liquid chromatography, reversed-phase high-performance liquid chromatography, chemiluminescence, capillary electrophoresis, and UV-visible spectrometry [8-12]. Despite the good selectivity and high accuracy of these methods, they are time-consuming, involve complicated operation, and are costly, thus limiting their practical application.

Photoelectrochemical (PEC) sensor is a new detection technology that has developed rapidly in

recent decades. By using light irradiation combined with electrochemical (EC) detection, PEC sensors combine the advantages of optical analysis and electrochemical sensing [13,14]. In addition, considering that the excitation light source of the sensor is completely separated from the photocurrent detection signal, the background value is greatly weakened in the detection process, thus allowing the PEC sensor to work under low noise and background current and providing ultra-high sensitivity [15-17]. Considering their advantages of simple instrumentation, rapid analysis, high sensitivity, and low cost, PEC sensors are widely used in biomedical, environmental monitoring, and other fields [18-20]. The properties of photoactive materials are very important for the performance of PEC sensing. Many materials with photoelectric properties, such as metal phthalocyanine, quantum dots (QDs), and TiO<sub>2</sub>, have been widely used in PEC sensors [21,22]. Among these materials, TiO<sub>2</sub> has attracted wide attention as an important semiconductor PEC material in PEC sensors because of its high activity, good photochemical stability, non-toxicity, large surface area, and economic advantages [23,24]. However, considering its wide band gap of ~3.2 eV for anatase form, bare TiO<sub>2</sub> can only be excited by UV light at wavelengths less than 387.5 nm (approximately 5% of the solar spectrum), and the visible light utilization rate is low, thus limiting its application in PEC sensing [25]. Narrow-band gap semiconductors, such as g-C<sub>3</sub>N<sub>4</sub> (~2.7 eV), CdS (~2.4 eV), CdTe (~1.7 eV), and PbS (~0.41 eV), diffuse the optical response to the visible region by combining with TiO<sub>2</sub> [26-29]. This property is attributed to the conduction band (CB) of these narrow-gap semiconductors with a value that is higher than that of TiO<sub>2</sub>; moreover, they can be used as sensitizers to facilitate the flow of photogenerated electrons from their CB to that of TiO<sub>2</sub>, thus promoting the charge separation and enhancing the PEC activity of TiO<sub>2</sub>-based composite materials [25].

Among these narrow band gap semiconductors, CdSe is a good sensitizer of TiO<sub>2</sub> because of its high light absorption efficiency and good electron mobility (800 cm<sup>2</sup> V<sup>-1</sup> s) [30]. This property can be attributed to the higher conduction band edge of CdSe than that of TiO<sub>2</sub>, thus allowing the transfer of photo-excited electrons to the conduction band of TiO<sub>2</sub>, and CdSe QDs have an adjustable quantum size effect [31-34]. CdSe QDs are excellent sensitizing substances with high chemical stability and electrochemical properties. In recent years, CdSe-sensitized TiO<sub>2</sub> has been extensively studied in photoelectrochemical solar cells [35-38]. However, its applications on PEC sensors are few.

Here, we report a self-assembly process (molten-salt-assisted self-assembly, MASA) synthesis of CdSe QDs sensitized TiO<sub>2</sub> photoanode on a fluorine-doped tin oxide (FTO)-coated glass (CdSe QDs-TiO<sub>2</sub>/FTO) and its application in PEC sensors to achieve sensitive detection of rutin. The experimental results show that the PEC sensor has excellent selectivity and good stability and has been successfully applied to the detection of rutin content in serum samples.

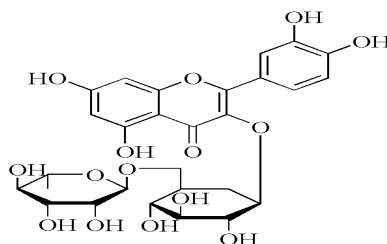


**Figure 1.** Chemical structure of rutin.

## 2. EXPERIMENTAL

### 2.1. Reagents and apparatus

Nano-TiO<sub>2</sub> (5–10 nm), titanium tetrabutoxide, sodium selenite (Na<sub>2</sub>SeO<sub>3</sub>), cadmium acetate dihydrate [Cd(CH<sub>3</sub>COO)<sub>2</sub>·2H<sub>2</sub>O], trisodium nitrilotriacetate (NTA), and sodium sulfide nonahydrate (Na<sub>2</sub>S·9H<sub>2</sub>O) were obtained from Aladdin Industrial Corporation (Shanghai, China). Rutin and nitric acid were provided by Kelong Chemical Reagent Plant (Chengdu, China). Zinc nitrate hexahydrate [Zn(NO<sub>3</sub>)<sub>2</sub>·6H<sub>2</sub>O], ethanol, and acetone were obtained from Sinopharm Group Chemical Reagent Co., Ltd. (Shanghai, China). Phosphate buffer saline (PBS, 0.1 M) was prepared using 0.1 M Na<sub>2</sub>HPO<sub>4</sub> and 0.1 M NaH<sub>2</sub>PO<sub>4</sub>. All reagents were of analytical grade and were not used for further purification. Double distilled water was used in all experiments. FTO-coated glass (50 mm×10 mm×1 mm, 15 Ω) was obtained from Yuanjingmei Glass Co., Ltd. (Foshan, China). Before use, the FTO electrode was ultrasonically cleaned in the order of distilled water, ethanol, acetone, ethanol, and distilled water for 10 min.

All PEC measurements were performed on a CHI 760E electrochemical workstation (Shanghai Chenhua Instrument Co., Ltd., Shanghai, China). The morphology of the material was characterized by scanning electron microscopy (SEM, Hitachi S-4800, Tokyo, Japan; 15 kV).

### 2.2 Preparation of CdSe QDs-TiO<sub>2</sub>/FTO

CdSe QDs-TiO<sub>2</sub>/FTO was synthesized using a previously reported method with some improvements [39]. Briefly, Nano-TiO<sub>2</sub> (3.0 g) was dispersed in 10 mL of absolute ethanol by stirring for 5 min. After sonication for 30 min, 0.5 mL of titanium tetrabutoxide and 1.0 g of 65% concentrated nitric acid were added, and the mixture was stirred for 5 min to obtain the TiO<sub>2</sub> monomer. Then, half of the FTO electrode was isolated by using a scotch tape, and 10 μL of TiO<sub>2</sub> monomer was evenly coated on the surface of the FTO electrode. The tape was removed, and the electrode was placed in a tube furnace and calcined at 500 °C for 2 h to obtain the TiO<sub>2</sub> film. Then, the prepared TiO<sub>2</sub> film was placed vertically into a mixed solution containing 0.1 M Na<sub>2</sub>SeO<sub>3</sub>, Cd(CH<sub>3</sub>COO)<sub>2</sub>·2H<sub>2</sub>O, and 0.2 M NTA and was allowed to stand for 3 h in the dark. Finally, the electrode was collected and washed with ethanol. After air-drying, the light-red CdSe QDs-TiO<sub>2</sub>/FTO photoanode was obtained.

### 2.3 Fabrication of the PEC sensor

ZnS treatments were employed prior to the PEC measurement of the electrode. A 0.1 M Zn(II) solution and 0.1 M S<sup>2-</sup> solution were prepared with Zn(NO<sub>3</sub>)<sub>2</sub>·6H<sub>2</sub>O and Na<sub>2</sub>S·9H<sub>2</sub>O, respectively. Subsequently, the CdSe QDs-TiO<sub>2</sub>/FTO electrode was immersed in the two solutions above in sequence for 30 s and washed with ethanol. This step is repeated thrice to ensure that all pore surfaces are covered with ZnS nanoparticles. This step aims to prevent the degradation of metal chalcogenides semiconductor and improve the stability of the photocurrent [40]. By using four different modified FTO electrodes (bare FTO, CdSe QDs/FTO, TiO<sub>2</sub> film/FTO, and CdSe QDs-TiO<sub>2</sub>/FTO electrode) as

the working electrode, Pt as the opposite electrode, and Ag/AgCl as the reference electrode, a three-electrode system was formed to construct the PEC sensor.

#### 2.4 Preparation of human serum samples

The human serum samples were obtained from Chongzuo People's Hospital (Guangxi, China). All experiments were performed in compliance with the relevant laws and institutional guidelines.

### 3. RESULTS AND DISCUSSION

#### 3.1 Characterization of the TiO<sub>2</sub> film and CdSe QDs-TiO<sub>2</sub> photoanode

The SEM image of the TiO<sub>2</sub> film and CdSe QDs-TiO<sub>2</sub> photoanode were shown in Figure 2. As shown in Figure 2A, the TiO<sub>2</sub> tended to aggregate as an irregular structure, and obvious voids were observed between structures, thus supporting the adsorption of CdSe QDs on the surface of TiO<sub>2</sub>. As shown in Figure 2B, many small particles were densely coated on the surface of the TiO<sub>2</sub> film, indicating that CdSe QDs were successfully attached to the TiO<sub>2</sub> and change its morphology and the CdSe QDs-TiO<sub>2</sub> photoanode was successfully prepared.

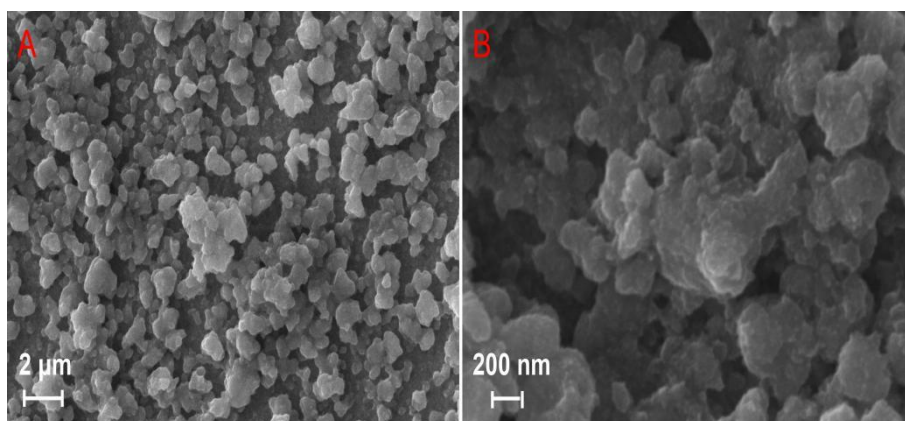


**Figure 2.** SEM image of the TiO<sub>2</sub> film (a) and CdSe QDs-TiO<sub>2</sub> photoanode.

#### 3.2 Characterization of PEC sensor

To evaluate the photoelectric activity of the material, we performed PEC tests on bare FTO electrode (curve a), CdSe QDs/FTO electrode (curve b), TiO<sub>2</sub> film/FTO electrode (curve c), and CdSe QDs-TiO<sub>2</sub>/FTO photoanode curve (curve d) in 0.1 M PBS buffer solution (pH 7.0) containing 12 μM of rutin. As shown in Figure 3A, curves a and b show a very low photocurrent of bare FTO and CdSe QDs/FTO, and curve c shows a relatively low photocurrent of TiO<sub>2</sub> film/FTO of 0.92 μA. CdSe QDs-TiO<sub>2</sub>/FTO (curve d) showed the largest photocurrent response (9.8 μA), indicating that CdSe QDs

sensitized TiO<sub>2</sub> by MASA greatly enhanced the photosensitization of TiO<sub>2</sub>. This result was obtained, because CdSe with a narrow band gap can transfer photo-excited electrons to TiO<sub>2</sub>, thus preventing photo-induced electron recombination, improving electron transfer efficiency, and resulting in a better photoelectric response than that of monomone.

Electrochemical impedance spectroscopy was used to evaluate the resistance and electron transfer capability of different modified electrodes. Figure 3B shows the Nyquist plot of bare FTO electrode (curve a), CdSe QDs/FTO electrode (curve b), TiO<sub>2</sub> film/FTO electrode (curve c), and CdSe QDs–TiO<sub>2</sub>/FTO (curve d) which obtained to 5 mM [Fe(CN)<sub>6</sub>]<sup>3-/4-</sup> in 0.1 M KCl solution. In the Nyquist impedance spectrum, the diameter of the semicircle in the high-frequency region is equivalent to the electron transfer impedance (Ret). As shown in Figure 3B, the CdSe QDs–TiO<sub>2</sub>/FTO photoanode shows the lowest Ret corresponding to the lowest charge transfer resistance compared with other electrodes. This result indicates that CdSe QDs were successfully loaded on the TiO<sub>2</sub> film, thus promoting charge separation and reducing the resistance.

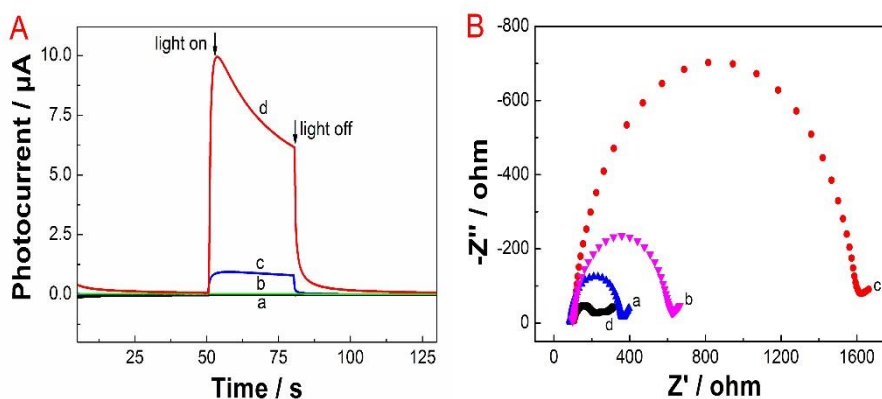
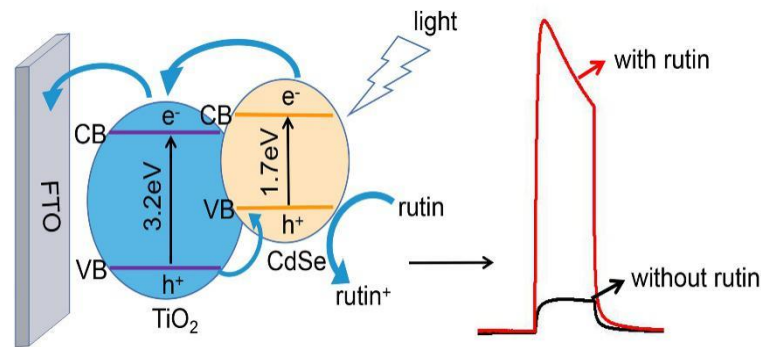


**Figure 3.** (A) Photocurrent responses and (B) Nyquist plots of bare FTO electrode (a), CdSe QDs/FTO electrode (b), TiO<sub>2</sub> film/FTO electrode (c), and CdSe QDs–TiO<sub>2</sub>/FTO electrode (d).

Based on the above results, scheme 1 proposed a mechanism for the detection of rutin on CdSe QDs–TiO<sub>2</sub>/FTO photoanode. Under visible light irradiation, the electrons of CdSe QDs with narrow band gap ( $\sim 1.70$  eV) are excited by photons and transfer from the valence band (VB) to the CB, forming electron ( $e^-$ )–hole ( $h^+$ ) pairs [28]. In addition, considering that CdSe can transfer photo-excited electron to the CB of TiO<sub>2</sub>, and the electrons on the CB of CdSe QDs are further transferred to the CB of TiO<sub>2</sub> [31]. The photoelectron transfer between CdSe QDs and TiO<sub>2</sub> effectively promotes charge separation and improves the electron transfer efficiency. Moreover, rutin as an electron donor can capture the holes of CdSe QDs and inject photoexcited electrons into the CB of TiO<sub>2</sub>, thus inducing  $e^-$  transfer to FTO electrode, while  $h^+$  reverse transfers to the VB of CdSe QDs, thereby suppressing electron-hole recombination and producing an enhanced photocurrent response [28,41,42].



**Scheme 1.** Mechanism of detection of rutin by PEC sensor.

### 3.3 Optimization of experimental conditions

The PEC response of CdSe QDs–TiO<sub>2</sub>/FTO photoanode to rutin in PBS buffer solution at pH 4.0–9.0 was investigated. As shown in Figure 4A, the photocurrent increased with increasing pH from 4.0 to 7.5 and then gradually decreased from pH 7.5 to 9.0. The maximum photocurrent was obtained at pH 7.5. Therefore, pH 7.5 was selected as the optimal pH for subsequent experiments. Then, the effect of different initialization voltage (voltage range –0.1 to 0.2 V) on the photocurrent response was studied. As shown in Figure 4B, the photocurrent response is maximum when the initialization voltage is 0.0 V. Therefore, the optimal initialization voltage of the PEC sensor was set to 0.0 V in this work.

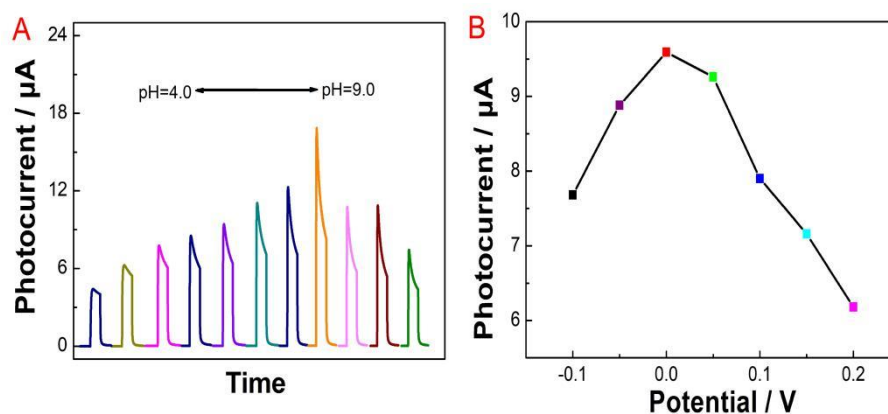


**Figure 4.** (A) Effect of different pH values (pH 4.0 ~ 9.0). (B) Effect of different initialization voltage (voltage range -0.1 ~ 0.2 V).

### 3.4 PEC detection of rutin

Figure 5 shows the effect of different concentrations of rutin on the photocurrent response of CdSe QDs–TiO<sub>2</sub>/FTO photoanode under optimal experimental conditions. It can be seen that the photocurrent increases with the increase of rutin concentration. In addition, the photocurrent has a linear relationship with the concentration in the range of 0.025–50.0 μM, and the linear equation is  $I=0.0191C + 0.1135$  ( $R^2=0.9955$ ). The limit of detection (LOD) was calculated to be 0.007 μM

(S/N=3). The proposed PEC sensor was compared with the previously reported sensors for the detection of rutin (Table 1). It can be seen that the CdSe QDs-TiO<sub>2</sub>/FTO provides a wide linear range and has a low LOD for rutin detection, which is comparable to other sensors.

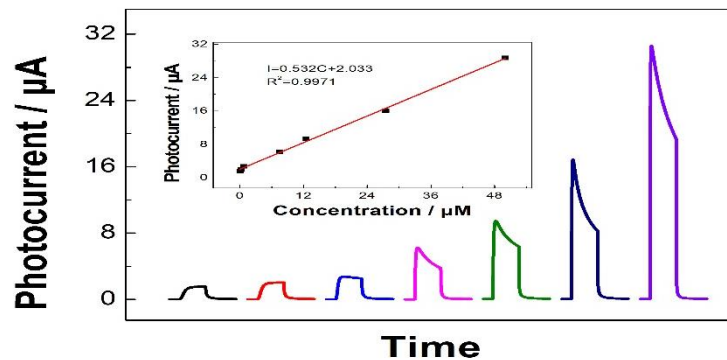


**Figure 5.** Photocurrent responses of CdSe QDs-TiO<sub>2</sub>/FTO in 0.1 M PBS buffer (pH 7.5) with 0.025–50.0 μM rutin. Inset: the corresponding linear equation.

**Table 1.** Comparison of different sensors for rutin determination.

Method	Modified electrodes	Technique	Linear range (μM)	LOD(μM)	References
EC	<sup>a</sup> ERGO/ <sup>b</sup> GCE	<sup>j</sup> DPV	0.47–12	0.018	[43]
EC	<sup>c</sup> ZIF-8-AB-CS/GCE	DPV	0.1–10	0.004	[44]
EC	<sup>d</sup> Cu <sub>2</sub> O-Au/NG/GCE	DPV	0.06–512.90	0.03	[45]
EC	<sup>e</sup> Co/ZIF-C/GCE	DPV	0.1–30	0.022	[46]
EC	<sup>f</sup> Pt@r-GO@MWCNTs/GCE	DPV	0.05–50	0.005	[47]
EC	<sup>g</sup> AuNPs-ZnS /GCE	<sup>k</sup> i-t	0.1–20	0.0153	[48]
PEC	<sup>h</sup> MIP/Bi <sub>2</sub> S <sub>3</sub> /ZnIn <sub>2</sub> S <sub>4</sub> / <sup>i</sup> ITO	i-t	0.01–100.0	0.003	[49]
PEC	CdSe QDs/TiO <sub>2</sub> /FTO	i-t	0.025–50.0	0.007	This work

<sup>a</sup>electrochemically reduced graphene oxide; <sup>b</sup>glassy carbon electrode; <sup>c</sup>zeolitic imidazolate framework-8 and acetylene black in the presence of chitosan; <sup>d</sup>Cu<sub>2</sub>O-Au/nitrogen-doped graphene nanocomposites; <sup>e</sup>cobalt decorated-nanoporous carbon; <sup>f</sup>platinum nanoparticle, reduced graphene oxide, multi-walled carbon nanotubes nanocomposite; <sup>g</sup>Au nanoparticles-loaded ZnS nanocomposites; <sup>h</sup>molecularly imprinted polymer; <sup>i</sup>Indium tin oxide glass; <sup>j</sup>differential pulse voltammetry; <sup>k</sup>current-time.

### 3.5 Selectivity, stability, and reproducibility of the PEC sensor

To investigate the selectivity of CdSe QDs-TiO<sub>2</sub>/FTO photoanode, some possible interferences and ions in actual samples were selected to evaluate their effect on the response of the sensor to the detection of rutin. The results (Table 2) show that the interfering substance have no significant interference to the photocurrent response of rutin at PEC sensor, and the relative error (Er) is less than

5%, indicating that the sensor has good selectivity.

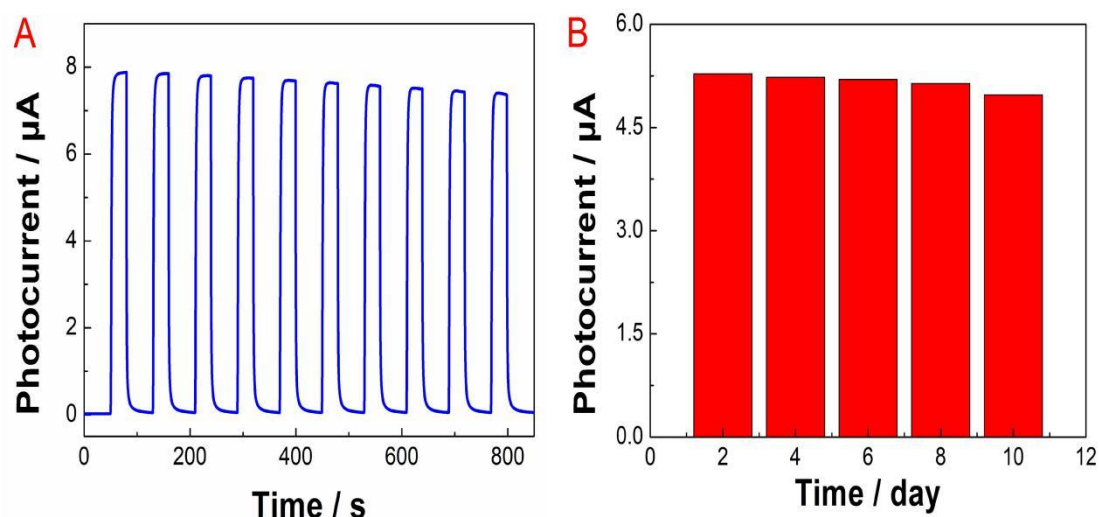


**Figure 6.** (A) Photocurrent response of the sensor after the continuous scanning light is turned on/off for 10 times. (B) Photocurrent response at the same rutin concentration for 10 days.

**Table 2.** Effects of interfering substances on the sensor to rutin.

Interferent	$n^a$	Er (%)	Interferent	$n^a$	Er (%)
Glucose	500	4.13	$\text{Al}^{3+}$	500	-3.27
Sucrose	200	-2.34	$\text{NO}_3^{2-}$	500	2.51
Glycine	200	-1.27	$\text{Ca}^{2+}$	500	-0.24
DL-alanine	100	4.59	$\text{Cl}^-$	100	-0.82
L-cysteine	100	3.49	$\text{Na}^+$	100	-0.82
Dopamine	50	2.36	$\text{Cu}^{2+}$	100	2.42
L-valine	50	4.59	$\text{Fe}^{3+}$	50	-1.33
Maltose	50	-2.18	$\text{Br}^-$	50	-1.06
Ascorbic acid	50	4.23	$\text{CO}_3^{2-}$	50	4.69
$\text{K}^+$	1,000	1.11	$\text{CH}_3\text{COO}^-$	50	1.45
$\text{Mg}^{2+}$	1,000	-0.48	$\text{SO}_4^{2-}$	50	-1.33

<sup>a</sup>Molar ratio(Interfering Substances / rutin).

In addition, to check the reproducibility of the PEC sensor, we prepared five modified



electrodes and performed measurements of the photocurrent to each one under optimal conditions with 4  $\mu\text{M}$  rutin. The relative standard deviation (RSD) of the photocurrent was 2%, indicating that the sensor has good reproducibility.

The stability of the sensor was also investigated. Figure 6A shows the short-term stability of the sensor and was investigated by circularly the light turned on 30 s and turned off for 50 s for 10 times, resulting in RSD of 2.01%. Furthermore, to evaluate the long-term stability, we stored the modified electrode at 4  $^{\circ}\text{C}$  for 10 days. The result is shown in Figure 6B. After 10 days, the sensor maintained 94% of the initial photocurrent. These results indicate that the sensor has good stability.

### 3.6 Detection of rutin in real samples

To examine the practical application of the PEC sensor for detecting rutin, we detected the human serum. The results are shown in Table 3. The recoveries ranged from 98.6% to 100.7%, and the RSD was less than 5%, indicating that the sensor has the potential for practical application.

**Table 3.** Analytical results for the determination of vanillin in human serum.

Sample	Original ( $\mu\text{M}$ )	Added ( $\mu\text{M}$ )	Found ( $\mu\text{M}$ )	Recovery (%)	RSD (%)
Serum 1	10	1.0	10.85	98.6%	3.92
Serum 2	10	2.0	11.92	99.3%	4.18
Serum 3	10	3.0	13.10	100.7%	4.22

## 4. CONCLUSIONS

In summary, a novel CdSe QDs–TiO<sub>2</sub>/FTO photoanode PEC sensor was fabricated and had been successfully developed for rutin determination. CdSe with a narrow band gap can transfer photo-excited electrons to TiO<sub>2</sub>, thus enhancing the photoelectric activity of TiO<sub>2</sub>. In comparison with CdSe QDs and TiO<sub>2</sub> monomer, the CdSe QDs–TiO<sub>2</sub>/FTO photoanode showed a stronger photocurrent response. The results show that under the optimal conditions, the proposed PEC sensor had excellent selectivity and good stability and exhibited a wide linear response range for rutin of 0.025–50.0  $\mu\text{M}$  with an LOD of 0.007  $\mu\text{M}$ . Moreover, the PEC sensor was successfully applied for the detection of rutin content in real sample.

## References

1. R. Mauludin, R.H. Müller and C.M. Keck, *Int. J. Pharm.*, 370 (2009) 202.
2. L.S. Chua, *J. Ethnopharmacol.*, 150 (2013) 805.
3. N. Gupta, S.K. Sharma, J.C. Rana and R.S. Chauhan, *J. Plant Physiol.*, 168 (2011) 2117.
4. A. Gęgotek, P. Domingues and E. Skrzydlewska, *J. Dermatol. Sci.*, 90 (2018) 241.

5. O.A. Chat, M.H. Najar, M.A. Mir, G.M. Rather and A.A. Dar, *J. Colloid Interf. Sci.*, 355 (2011) 140.
6. N.A. Al-Shabib, F.M. Husain, I. Ahmad, M.S. Khan, R.A. Khan and J.M. Khan, *Food Control*, 79 (2017) 325.
7. S. Sharma, A. Ali, J. Ali, J.K. Sahni and S. Baboota, *Expert Opin. Investig. Drugs*, 22 (2013) 1063.
8. C. H. Wang, Y. X. Wang and H. J. Liu, *J. Pharm. Anal.*, 1 (2011) 291.
9. V. Kuntičić, N. Pejić, B. Ivković, Z. Vujić, K. Ilić, S. Mičić and V. Vukojević, *J. Pharm. Biomed. Anal.* 43 (2007) 718.
10. H. Wu, M. Chen, Y. Fand, F. Elsebaei and Y. Zhu, *Talanta*, 88 (2012) 222.
11. G. Chen, H. Zhang and J. Ye, *Anal. Chim. Acta*, 423 (2000) 69.
12. A. Gong, W. Ping, J. Wang and X. Zhu, *Spectrochim. Acta Part A: Mol. Biomol. Spectrosc.*, 122 (2014) 331.
13. L. Zhong, X. Li, R. Liu, X. Wei and J. Li, *Analyst*, 144 (2019) 3405.
14. W. Ma, D. Han, S. Gan, N. Zhang, S. Liu, T. Wu, Q. Zhang, X. Dong and L. Niu, *Chem. Commun.*, 49 (2013) 7842.
15. R.M. Mazhabi, L. Ge, H. Jiang and X. Wang, *Biosens. Bioelectron.*, 107 (2018) 54.
16. X. Wang, H. Deng, C. Wang, Q. Wei, Y. Wang, X. Xiong, C. Li and W. Li, *Analyst*, 145 (2020) 1302.
17. S. Wu, H. Huang, M. Shang, C. Du, Y. Wu and W. Song, *Biosens. Bioelectron.*, 92 (2017) 646.
18. W.W. Zhao, J.J. Xu and H.Y. Chen, *Chem. Soc. Rev.*, 44 (2015) 729.
19. Y. Cao, L. Wang, C. Wang, X. Hu, Y. Liu and G. Wang, *Electrochim. Acta*, 317 (2019) 341.
20. J. Peng, W. Zhuge, Y. Huang, C. Zhang and W. Huang, *Bull. Korean Chem. Soc.*, 40 (2019) 214.
21. J. Peng, Q. Huang, Y. Liu, F. Liu, C. Zhang and Y. Huang, *J. Chin. Chem. Soc.*, 66 (2019) 1.
22. X. Zhang, Y. Guo, M. Liua and S. Zhang, *RSC Adv.*, 3 (2013) 2846.
23. T.L. Thompson and J.T. Yates, *Chem. Rev.*, 106 (2006) 4428.
24. H. Li, J. Li, Y. Zhu, W. Xie, R. Shao, X. Yao, A. Gao and Y. Yin, *Anal. Chem.*, 90 (2018) 5496.
25. F.X. Wang, C. Ye, S. Mo, L.L. Liao, X.F. Zhang, Y. Ling, L. Lu, H.Q. Luo and N.B. Li, *Analyst*, 143 (2018) 3399.
26. P. Liu, X. Huo, Y. Tang, J. Xua, X. Liu and D.K.Y. Wong, *Anal. Chim. Acta*, 984 (2017) 86.
27. L. Ding, C. Ma, L. Li, L. Zhang and J. Yu, *J. Electroanal. Chem.*, 783 (2016) 176.
28. D. Fan, X. Ren, H. Wang, D. Wu, D. Zhao, Y. Chen, Q. Wei and B. Du, *Biosens. Bioelectron.*, 87 (2017) 593.
29. Y. Yan, Q. Liu, X. Du, J. Qian, H. Mao and K. Wang, *Anal. Chim. Acta*, 853 (2015) 258.
30. B. Chong, W. Zhu, Y. Liu, L. Guan and G.Z. Chen, *J. Mater. Chem. A*, 4 (2016) 1336.
31. G.K. Larsen, B.C. Fitzmorris, C. Longo, J.Z. Zhang and Y. Zhao, *J. Mater. Chem.*, 22 (2012) 14205.
32. P. Wang, D. Li, J. Chen, X. Zhang, J. Xian, X. Yang, X. Zheng, X. Li and Y. Shao, *Appl. Catal. B: Environ.*, 217 (2014) 160.
33. J.H. Bang and P.V. Kamat, *Adv. Funct. Mater.*, 20 (2010) 1970.
34. J. Hensel, G. Wang, Y. Li and J.Z. Zhang, *Nano Lett.*, 10 (2010) 478.
35. R. Narayanan, M. Deepa and A.K. Srivastava, *Phys. Chem. Chem. Phys.*, 14 (2012) 767.
36. S.K. Kim, M.K. Son, S. Park, M.S. Jeong, K. Prabakar and H.J. Kim, *Electrochim. Acta*, 118 (2014) 118.
37. L.H. Lai, W. Gomulya, L. Protesescu, M.V. Kovalenkobc and M.A. Loi, *Phys. Chem. Chem. Phys.*, 16 (2014) 7531.
38. Q. Qiu, P. Wang, L. Xu, D. Wang, Y. Lin and T. Xie, *Phys. Chem. Chem. Phys.*, 19 (2017) 15724.
39. M.Y. Yaman, A.S. Han, J. Bandara, C. Karakaya and Ö. Dag, *ACS Omega*, 2 (2017) 4982.
40. B. Chong, W. Zhu and X. Hou, *J. Mater. Chem. A*, 5 (2017) 6233.
41. W. Tu, J. Lei, P. Wang and H. Ju, *Chem. Eur. J.*, 17 (2011) 9440.
42. X. Chen, J. Li, G. Pan, W. Xu, J. Zhu, D. Zhou, D. Li, C. Chen, G. Lu and H. Song, *Sensor. Actuat. B: Chem.*, 289 (2019) 131.

43. P. Zhang, Y.Q. Gou, X. Gao, R.B. Bai, W.X. Chen, B.L. Sun, F.D. Hu and W.H. Zhao, *J. Pharm. Anal.*, 6 (2016) 80.
44. Y. Jin, C. Ge, X. Li, M. Zhang, G. Xu and D. Li, *RSC Adv.*, 8 (2018) 32740.
45. S. Li, B. Yang, C. Wang, J. Wang, Y. Feng, B. Yan, Z. Xiong and Y. Du, *J. Electroanal. Chem.*, 786 (2017) 20.
46. A. Şenocak, A. Khataee, E. Demirbas and E. Doustkhah, *Sensor. Actuat. B: Chem.*, 312 (2020) 127939.
47. J. Wang, B. Yang, S. Li, B. Yan, H. Xu, K. Zhang, Y. Shi, C. Zhai and Y. Du, *J. Colloid Interf. Sci.*, 506 (2017) 329.
48. J. Xi, H. Wang, B. Zhang, F. Zhao and B. Zeng, *Sensor. Actuat. B: Chem.*, 320 (2020) 128409.
49. R. Xing, X. Zhao, Y. Liu, J. Liu, B. Liu, Y. Ren, S. Liu and L. Mao, *J. Nanosci. Nanotechnol.*, 18 (2018) 4651.

© 2021 The Authors. Published by ESG ([www.electrochemsci.org](http://www.electrochemsci.org)). This article is an open access article distributed under the terms and conditions of the Creative Commons Attribution license (<http://creativecommons.org/licenses/by/4.0/>).